Shear-induced particle rotation and its effect on electrorheological and dielectric properties in cellulose suspension

Y. Misono and K. Negita
Department of Chemistry, Faculty of Science, Fukuoka University, Nanakuma 8-19-1, Jonan-ku, Fukuoka 814-0180, Japan
(Received 7 April 2004; published 28 December 2004)

Electrorheological (ER) and dielectric properties under high electric fields were measured simultaneously on hydroxypropylcellulose suspension. When measuring these properties as a function of frequency of the electric field, we found a positive peak in each spectrum of the ER effect and the first-order dielectric permittivity while a negative one in the spectrum of the third-order dielectric permittivity with these peak frequencies nearly equal to (shear rate)$/4\pi$. Referring to the well-known results for the particle rotation in the sheared suspension, it is suggested that the observed peaks are due to shear-induced particle rotation and the rotation occurs even under high electric field. On the basis of these results, effects of the particle rotation on the ER and the dielectric properties are discussed.

DOI: 10.1103/PhysRevE.70.061412 PACS number(s): 83.80.Hj, 83.60.Np, 83.50.Ax, 77.84.Nh

I. INTRODUCTION

If an electric field of a few kV/mm is applied to an electrorheological (ER) suspension composed of dielectric particles and electrically nonconducting liquids, a large increase in the apparent viscosity is observed [1]. Owing to its large and fast rheological change, the ER suspensions have been suggested to be potential functional materials applicable to some mechanical devices, such as ER clutch, ER shock-absorber, and ER valve [2]. The ER effect occurs as a result of a field-induced structural change; the application of the electric field induces an interfacial polarization on the particle, and the resultant dipole-dipole interaction between the particles gives rise to chainlike and/or column structures responsible for the rheological change [3–6]. The induced polarization, thus, plays an important role for the ER effect, and many studies have been made to clarify the relationships between the dielectric properties and the ER effect [3–9]. Of these studies, frequency dependence of the ER and the dielectric properties has given us important information. If the frequency of the electric field is increased, the ER effect in most ER fluids decreases above a certain frequency, which is consistently interpreted in terms of the relaxation effect of the interfacial polarization [3,7–9]. Furthermore, the strength of the ER effect has been suggested to be associated with the relaxation strength $\Delta\varepsilon' = \varepsilon_s - \varepsilon_h'$, where ε_s is the static dielectric permittivity and ε_h' is the dielectric permittivity at high frequency, where the contribution from the interfacial polarization disappears [8,9]. In addition, it is indicated that if the ER effect is measured as a function of the frequency of the electric field, a peak appears at a certain frequency in the ER effect. This phenomenon, ER resonance, is observed in some suspensions showing a weak ER effect, such as the TiO_2 suspension, and is understood to occur as a result of the shear-induced particle rotation [10]. The ER mechanism, thus, has been clarified in some aspects, but its understanding is not enough to get much stronger ER fluids. For further understanding of the ER mechanism, the dielectric measurement will continue to play an important role. Up to now, however, most of the dielectric properties have been measured at low fields in the absence of shear flow. If we consider that the ER effect appears at high electric fields in the presence of shear flow, dielectric measurement under both high electric field and shear flow would be desirable because it is expected that the dielectric property in such a condition would be different from that under low electric field and no shear flow. In the present study, simultaneous measurements of the ER and dielectric properties were made on hydroxypropylcellulose (HOPC) suspension. In our measurements on the frequency dependence of the ER effect and the dielectric properties, a resonance peak was observed in each spectrum of the ER effect and first- and third-order dielectric permittivities. From the relationship between the peak frequencies and the shear rates, it is suggested that a shear-induced particle rotation occurs in the ER suspension even at high electric fields. On the basis of these results, effects of the particle rotation on the ER and the dielectric properties are discussed.

II. EXPERIMENTAL

The HOPC suspension (20 vol%) was prepared by dispersing HOPC (H0475, Tokyo Kasei, Japan) particles into 50 cS silicone oil (TSF451-50, Toshiba Silicone, Japan). The particles are 50 μm in average diameter and contain about 2 wt% of water. The ER and the dielectric properties were measured simultaneously with a double cylinder type of viscometer [11]. A small ac voltage from a function-generator (1946, NF Electric Instr., Japan) was amplified up to a few kV with a high-voltage amplifier (664, Trek, USA). The high voltage thus obtained was applied to the gap (1 mm) between the inner and the outer cylinders of the viscometer to generate a high electric field ($E = E_0 e^{i\omega t}$) perpendicular to the flow direction. The dielectric property of the ER fluids at high fields is generally nonlinear. To obtain the harmonics of the complex electric displacements of $D^*(\omega)$ and $D^*(3\omega)$, phase sensitive detection of the current passing through the fluid was made with a lock-in amplifier (7260, EG&G Instr., USA). In the nonlinear dielectric response, the electric displacements are expressed by following equations: $D^*(\omega)$

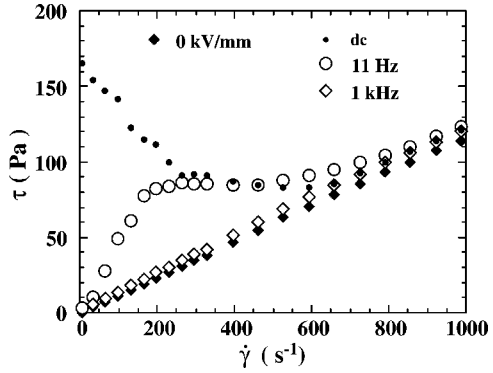

FIG. 1. Changes in rheology (shear stress vs shear rate) under application of electric field (2 kV/mm). Results under no electric field, dc field, and ac fields (11 Hz and 1 kHz) are given.

$=\varepsilon_1^* E_0 +$(higher-order terms) and $D^*(3\omega)=(\varepsilon_3^* E_0^3)/4$ +(higher-order terms), where ε_1^* and ε_3^* are first- and third-order complex dielectric constants, respectively, and E_0 is the amplitude of the electric field [12]. In the present study, neglecting the higher-order terms of the above equations, apparent first- and third-order dielectric constants were obtained. All the measurements were made at room temperature (300 K). The electric field strength is expressed in rms.

III. RESULTS

A. ER effect

Changes in the shear stress versus shear rate relationships on application of dc and ac electric fields (2 kV/mm) are given in Fig. 1. In the absence of the electric field, the flow is Newtonian with the shear stress being proportional to the shear rate. The application of dc field results in an increase of the shear stress with its magnitude decreasing with increase in the shear rate. On the other hand if ac fields are applied, the ER behavior is largely modified with its behavior depending on the frequency of the electric field. At 11 Hz, the induced shear stress ($\Delta\tau$) has a peak at a certain shear rate and becomes smaller at both lower and higher shear rate regions, while at 1 kHz the ER effect is small at all shear rates.

To make clear how the induced shear stress $\Delta\tau$ depends on the electric field strength E, $\Delta\tau$ is measured as a function of E at a shear rate of 329.5 s^{-1} (Fig. 2). As shown in Fig. 2(a) (linear plot), under the dc field $\Delta\tau$ once decreases to negative values and then increases with increase in the electric field strength, which is contrasted to the monotonous increases in $\Delta\tau$ caused by the ac fields. Although the origin of the negative ER effect under the dc field is not clear at present, the Quincke rotation of the particle would be a possible mechanism; it is reported that the Quincke rotation is easier to occur in a dc field than in an ac field to give rise to a negative ER effect [13]. In Fig. 2(b), log-log plots for $\Delta\tau$ versus E are given. The induced shear stress $\Delta\tau$ is nearly proportional to E^2 at high fields, as expected from the interaction between the induced dipoles, but at low fields $\Delta\tau$ depends on E with the coefficient $m(\Delta\tau \propto E^m)$ larger than 2.

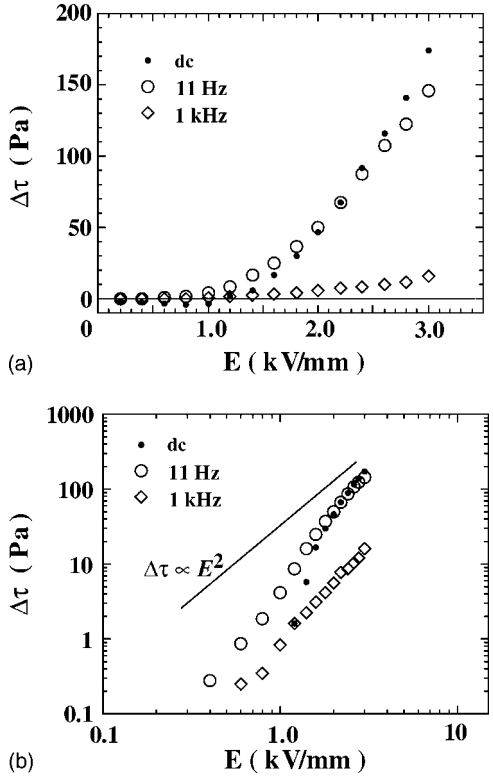

FIG. 2. Induced shear stress (measured at a shear rate of 329.5 s^{-1}) vs amplitude of the electric field. Results under dc field and ac fields (11 Hz and 1 kHz) are given: (a) linear plot and (b) log-log plot. The straight line in Fig. 2(b) represents a relation of $\Delta\tau \propto E^2$.

The deviation from $\Delta\tau \propto E^2$ is larger under the dc field compared to those under the ac fields, which can be understood if we consider that the Quincke rotation at low fields is gradually suppressed to form a chainlike structure with increase in the electric field strength. To verify whether the Quincke rotation is responsible for these behaviors, further investigation is necessary.

To know the frequency dependence of the ER effect, $\Delta\tau$ is measured as a function of frequency of the electric fields (1.0 and 2.0 kV/mm) at a constant shear rate 329.5 s^{-1} (Fig. 3). As obvious from this figure, a peak is observed, followed by a steep decrease in $\Delta\tau$ above the peak frequency. The peak position is not affected by the change in the electric field strength, although the height of the peak is affected. To understand the origin of the peak, varying the shear rate, frequency dependence of $\Delta\tau$ is measured at 2 kV/mm (Fig. 4). As the figure shows, the peak shifts to higher frequencies with increase in the shear rate. Such a behavior has been reported in TiO_2 suspension and has been interpreted to occur as a result of the ER resonance; matching of the frequency of the electric field to that of the shear-induced particle rotation causes a peak in the ER effect [10]. The observed peaks in Figs. 3 and 4, thus, can be attributed to the shear-induced particle rotation.

B. dc conductivity

The dc current density J passing through the suspension is measured at 2 kV/mm as a function of the shear rate (Fig.

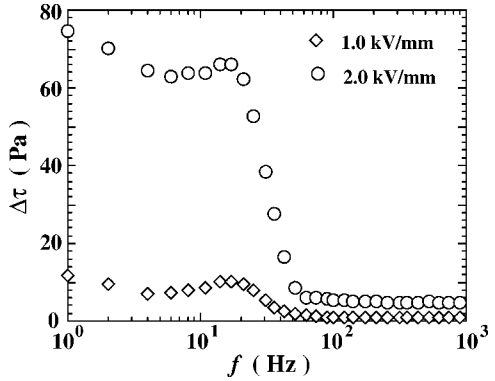

FIG. 3. Induced shear stress (measured at a shear rate of 329.5 s^{-1}) vs frequency of the electric field at 1.0 kV/mm and 2.0 kV/mm.

5). With an increase in the shear rate, the current density decreases and becomes almost constant above ~700 s^{-1}. This behavior is similar to that of the induced shear stress under the dc field (Fig. 1), indicating that a same mechanism may govern the shear-rate dependence of the dc conductivity and the ER effect. To make clear the *J-E* relationship, dc current density is measured as a function of the electric field strength at a constant shear rate 329.5 s^{-1}. As Fig. 6 shows, the current density increases nonlinearly with the electric field strength with a relation of $J \propto E^{1.6}$. The nonlinear electrical conduction is generally observed in ER active suspensions with the nonlinear coefficient $\alpha(J \propto E^{\alpha})$ less than about 5 (Refs. [3,14–16]). The mechanism of the nonlinear conduction of the ER suspension is not well understood, but it reflects that with an increase in the electric field strength the interparticle attraction becomes stronger, giving rise to an enhancement of the interparticle charge transfer.

C. Dielectric permittivity

Varying the shear rate, the dielectric permittivity at 2 kV/mm is measured at 11 Hz and 1 kHz (Fig. 7). In the case of 11 Hz, a peak is observed around 140 s^{-1}, whereas no peak in the case of 1 kHz. These behaviors are similar to

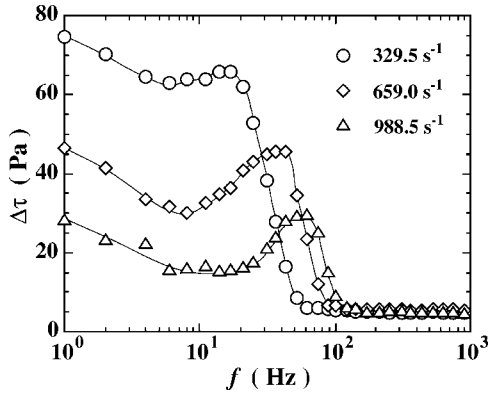

FIG. 4. Induced shear stress (measured at a shear rate of 329.5 s^{-1}) vs frequency of the electric field (2.0 kV/mm) at some shear rates. Lines are drawn to guide the eye.

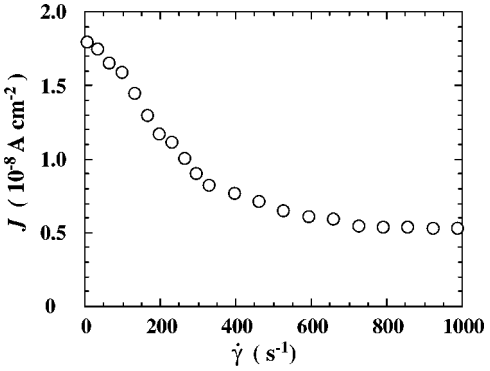

FIG. 5. dc current density vs shear rate, measured at an electric field of 2.0 kV/mm.

those observed in the induced shear stress $\Delta\tau$ in Fig. 1. In order to make clear the origin of the peak, varying the shear rate, first- and third-order dielectric permittivities are measured as a function of the frequency of the electric field. As shown in Fig. 8(a), in the absence of the shear flow ε_1' decreases monotonously with increase in the frequency, but under the shear flow a clear positive peak is observed in ε_1' with its peak position depending on the shear rate. This figure also shows that the peak position shifts to higher frequency if the shear rate is increased. While in ε_3', Fig. 8(b), a negative peak is observed under a shear flow with a similar shear rate dependence of the peak position to that of ε_1'. Under no shear flow, ε_3' is almost zero without depending on the frequency of the electric field, which clearly indicates that the observed peaks are caused by the steady shear flow. When the electric field strength is varied, the peaks in dielectric permittivities are affected, which are depicted in Fig. 9, with first- and third-order dielectric permittivities given in Figs. 9(a) and 9(b), respectively. With an increase in the electric field strength, ε_1' increases nonlinearly in the low-frequency region with small change in the shape of the peak, while the peak in ε_3' becomes smaller as recognized from this figure.

IV. DISCUSSION

As mentioned above, frequency dependence of the ER and the dielectric properties of the HOPC suspension is char-

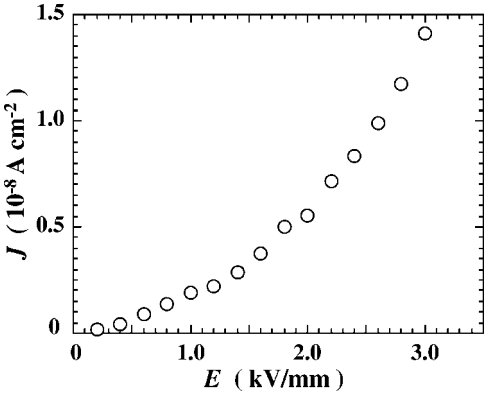

FIG. 6. dc current density vs amplitude of the electric field, measured at a shear rate of 329.5 s^{-1}.

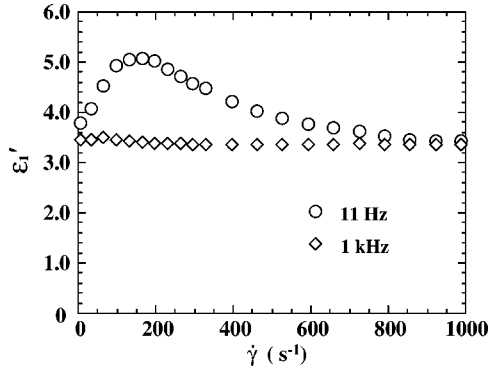

FIG. 7. Dielectric permittivity vs shear rate measured at an electric field of 2 kV/mm. Results at 11 Hz and 1 kHz are given.

acterized by the peaks, which depend on the shear rate. To make clear the origin of these peaks, the peak frequencies f_p of the ER and the dielectric permittivities are plotted against shear rate $\dot{\gamma}$ (Fig. 10). A solid line in this figure represents a well-known relationship of $f=\dot{\gamma}/4\pi$ [17,18]; in the absence of the electric field, if a steady shear flow is applied to a suspension, then a particle rotation occurs with its rotational frequency equal to $\dot{\gamma}/4\pi$. As can be seen from this figure, the peak frequencies of the ER effect and the first- and third-order dielectric permittivities are well characterized by $f_p \approx \dot{\gamma}/4\pi$, suggesting that the steady shear flow induces a particle rotation even at high fields, where the chainlike and/or column structures are formed. The facts that the peak frequencies are somewhat lower than (shear rate)$/4\pi$ can be understood as a consequence of a suppression of the particle rotation under the high electric field [8].

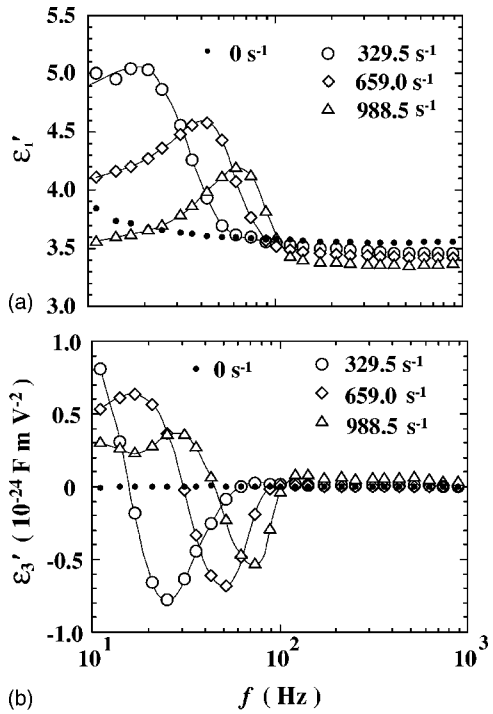

FIG. 8. Dielectric permittivities vs frequency of the electric field (2.0 kV/mm) at some shear rates. (a) first-order dielectric permittivity and (b) third-order dielectric permittivity. Lines are drawn to guide the eye.

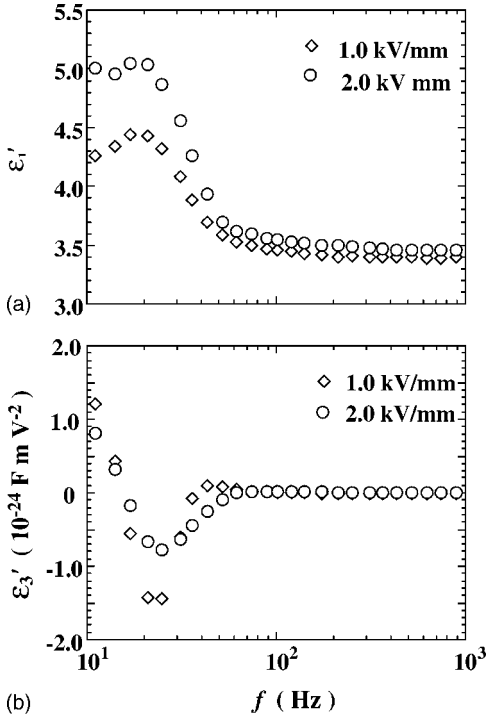

FIG. 9. Dielectric permittivities vs frequency of the electric field measured at shear rate of 329.5 s^{-1}. Results at 1.0 kV/mm and 2.0 kV/mm are given: (a) first-order dielectric permittivity and (b) third-order dielectric permittivity.

In order to clarify the effect of the particle rotation on the ER effect and the dielectric permittivities, an interfacial polarization under influence of particle rotation is considered. Here, it is assumed the particle rotates around the x-axis at an angular frequency of Ω and the electric field $E=E_0\exp(i\omega t)$ is applied along the z-axis as depicted in Fig. 11. As has been well known, under a shear flow the angular frequency Ω is related to the shear rate $\dot{\gamma}$ as $\Omega=\dot{\gamma}/2$. In such a condition, the polarizations are induced not only along the z-axis, but also along the y-axis. Of these polarizations, the polarization along the electric field P_z is so important for the ER effect that we consider only P_z in the present analysis. The angular frequency (ω) dependence of P_z can be expressed by Eq. (1) [19,20]

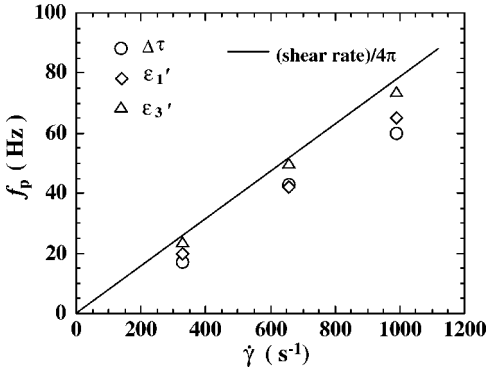

FIG. 10. Peak frequencies of the ER effect and first- and third-order dielectric permittivities vs shear rate. The solid line represents a relation of $f=$(shear rate)$/4\pi$.

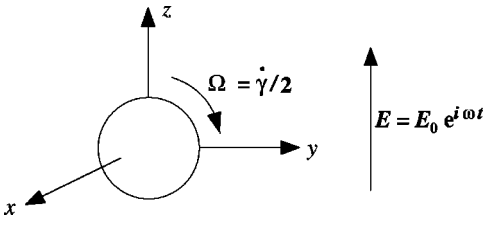

FIG. 11. Coordinate system specifying the directions of the particle rotation and the electric field.

$$P_z^*(\omega) = \frac{1+\omega\tau_r}{1-(\omega^2-\Omega^2)\tau_r^2+2i\omega\tau_r}\Delta\alpha E_0. \quad (1)$$

Here, $\Delta\alpha$ is the difference in the polarizability between $\omega=0$ and $\omega=\infty$, and τ_r is the relaxation time of the interfacial polarization. In Eq. (1), $P_z^*(\omega)$ is composed of real and imaginary parts, of which the real part $P_z'(\omega)$ corresponds to the dielectric permittivity and is associated with the magnitude of the ER effect. If we make the angular frequency and the relaxation time dimensionless, then $\tilde{\omega}=\omega/\Omega$ and $\tilde{\tau}_r=\tau_r\Omega$, $P_z'(\omega)$ is converted to $P_z'(\tilde{\omega})$ as Eq. (2),

$$P_z'(\tilde{\omega}) = \frac{1+(\tilde{\omega}^2+1)\tilde{\tau}_r^2}{[1-(\tilde{\omega}^2-1)\tilde{\tau}_r^2]^2+4\tilde{\omega}^2\tilde{\tau}_r^2}\Delta\alpha E_0. \quad (2)$$

The profile of $P_z'(\tilde{\omega})$ under variation of $\tilde{\tau}_r$ is given in Fig. 12. As obvious from this figure, if $\tilde{\tau}_r \ll 1$, $P_z'(\tilde{\omega})$ shows a relaxation type of spectrum; a dielectric dispersion appears characterized by the relaxation time $\tilde{\tau}_r$. While if $\tilde{\tau}_r \gg 1$, the spectrum changes to a resonance type with its peak at $\tilde{\omega}\approx 1$ and the magnitude of the polarization is considerably reduced as recognized in this figure. Comparing these calculated results to the observed ER effects (Figs. 3 and 4) and the dielectric permittivities [Figs. 8(a) and 9(a)], we find that $\tilde{\tau}_r$ is in the range of $1<\tilde{\tau}_r<10$ when the shear rate is 329.5 s^{-1}. This indicates that in the HOPC suspension the relaxation time of the interfacial polarization is not so fast, leading to the resonance type of spectra in the ER effect and the dielectric permittivities. The peaks in the ER effect (Fig. 1) and the dielectric permittivity (Fig. 7) obtained at 11 Hz can also be interpreted to occur as a result of the particle rotation, which is evidenced by the fact that these peaks appear at a shear rate of about $4\pi f$. In addition, the shear rate dependence of the ER effect under the dc field (Fig. 1) can be qualitatively understood if we consider that Eq. (2) is reduced to $P_z(0)=\Delta\alpha E_0(1+\tilde{\tau}_r^2)^{-1}$ at $\tilde{\omega}=0$. It is also expected that the shear rate dependence of the dc current (Fig. 5) is due to the shear-induced particle rotation, since its shear rate dependence is similar to that of the ER effect under the dc field (Fig. 1). In such a way, the ER effect and the dielectric permittivities are qualitatively understood on the basis of Eq. (2) derived as a linear dielectric permittivity. However, at high electric field, nonlinear effects appear; the dielectric permittivity and the relaxation time of the interfacial polarization vary with the electric field strength. For quantitative understanding of the ER and the dielectric properties, a theoretical approach including the nonlinear effects is necessary.

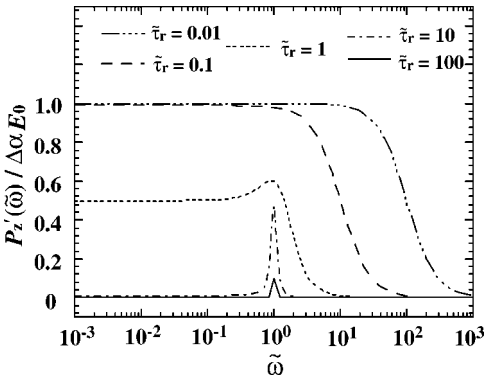

FIG. 12. Calculated results for the polarization P_z' vs dimensionless angular frequency $\tilde{\omega}=\omega/\Omega$ under variation of dimensionless relaxation time $\tilde{\tau}_r=\tau_r\Omega$.

As mentioned above, the anomalous behaviors of the ER effects, dielectric permittivities, and electrical conductivity in HOPC suspension can be almost consistently interpreted in terms of shear-induced particle rotation. The effect of the particle rotation, however, is modified if the relaxation time τ_r becomes shorter. In other suspensions, such as carbon and starch suspensions [21,22], the ER effect and the first-order dielectric permittivity show relaxation type of spectra without giving the resonance peak as observed in HOPC suspension. In these suspensions, the relaxation time of the interfacial polarization is shorter, i.e. $\tilde{\tau}_r<1$, which gives rise to a relaxation type of polarization as shown Fig. 11. However, in the third-order dielectric permittivity, a resonance-type spectrum as in Fig. 8(b) is observed in each suspension, indicating that the shear-induced particle rotation occurs also in these suspensions.

The higher-order dielectric permittivities, which are studied only in limited research fields, give us meaningful information [12,23–27]. For instance, in the third-order dielectric permittivity, not only the polarization but also some other order coupling to the polarization is responsible for the spectrum, giving us more information on the microscopic environment of the polarization than the first-order permittivity [24,27]. Such a sensitive property of third-order permittivity may lead to the detection of the resonance peak caused by the shear-induced particle rotation. For the negative resonance peak in the third-order dielectric permittivity, following qualitative explanation may be possible. When an electric field is increased, the interparticle dipolar interaction becomes stronger, resulting in the suppression of the shear-induced particle rotation (i.e., reduction of the dielectric susceptibility associated with the particle rotation). This phenomenon occurs equivalently under the reversed field. Therefore, the dielectric permittivity under the electric field is expressed as $\varepsilon(E)=\varepsilon_1+\varepsilon_3E^2$ with $\varepsilon_3<0$. For understanding the exact mechanism for the resonance peak in the third-order dielectric permittivity, theoretical analysis is necessary and now in progress.

The shear-induced particle rotation under high electric fields, thus, is recognized in most of the ER suspensions,

indicating that it would be a general property of the ER suspension. As described above, the particle rotation thus induced influences the magnitude of the interfacial polarization along the electric field and, hence, the strength of the ER effect. For developing higher-performance ER fluids, it would be necessary to take into account the effect of the shear-induced particle rotation.

ACKNOWLEDGMENT

This study was supported by special coordination funds for promoting science and technology from the Ministry of Education, Culture, Sports, Science, and Technology of Japan, to whom we are deeply indebted.

[1] W. M. Winslow, J. Appl. Phys. **20**, 1137 (1949).
[2] D. L. Hartstock, R. F. Novak, and G. J. Chaundy, J. Rheol. **35**, 1305 (1991).
[3] D. K. Klass and T. W. Matrinek, J. Appl. Phys. **38**, 67 (1967); **38**, 75 (1967).
[4] A. P. Gast and C. F. Zukoski, Adv. Colloid Interface Sci. **30**, 153 (1989).
[5] H. Block and J. P. Kelly, J. Phys. D **21**, 1661 (1988).
[6] D. J. Klingenberg, F. van Swol, and C. F. Zukoski, J. Chem. Phys. **91**, 7888 (1989).
[7] H. Uejima, Jpn. J. Appl. Phys. **11**, 319 (1972).
[8] K. Negita and Y. Ohsawa, J. Phys. II **5**, 883 (1995).
[9] T. Hao, A. Kawai, and F. Ikazaki, Langmuir **14**, 1256 (1998).
[10] K. Negita and Y. Ohsawa, Phys. Rev. E **52**, 1934 (1995).
[11] K. Negita, Netsu Sokutei **22**, 137 (1995).
[12] Y. Kimura and R. Hayakawa, Jpn. J. Appl. Phys., Part 1 **32**, 4571 (1993).
[13] L. Lobry and E. Lemaire, J. Electrost. **47**, 61 (1999).
[14] F. E. Filisko and L. H. Radzilowski, J. Rheol. **34**, 539 (1990).
[15] H. Conrad and Y. Chen, in *Progress in Electrorheology*, edited by K. O. Havelka and F. E. Filisko (Plenum, New York, 1995), pp. 55–85.
[16] C. Boissy, P. Atten, and J.-N. Foulc, in *Electro-Rheological Fluids, Magneto-Rheological Suspensions and Associated Technology*, edited by W. A. Bullough (World Scientific, Singapore, 1996), pp. 156–165.
[17] G. B. Jeffrey, Proc. R. Soc. London, Ser. A **102**, 161 (1922).
[18] H. Block, K. M. W. Goodwin, E. M. Gregson, and S. M. Walker, Nature (London) **275**, 633 (1978).
[19] H. Block, E. Kluk, J. McConell, and B. K. Scaife, J. Colloid Interface Sci. **101**, 320 (1984).
[20] J. Hemp, Proc. R. Soc. London, Ser. A **434**, 397 (1991).
[21] K. Negita, Y. Misono, and J. Shinagawa, *Proceeding of International Symposium on Innovative Materials Processing by Controlling Chemical Reaction Field (IMP 2002)* (2002), p. 64 (unpublished).
[22] Y. Inamasu, Master's thesis, Fukuoka University 2004 (unpublished).
[23] S. Ikeda, H. Kominami, K. Koyama, and Y. Wada, J. Appl. Phys. **62**, 3339 (1987).
[24] T. Furukawa and K. Matsumoto, Jpn. J. Appl. Phys., Part 1 **31**, 840 (1992).
[25] H. Orihara, A. Fukase, S. Izumi, and Y. Ishibashi, Ferroelectrics **147**, 411 (1993).
[26] H. Orihara and Y. Ishibashi, J. Phys. Soc. Jpn. **62**, 489 (1993).
[27] K. Obayashi, H. Orihara, and Y. Ishibashi, J. Phys. Soc. Jpn. **64**, 3188 (1995).